HHS Public Access

Author manuscript

Cell Host Microbe. Author manuscript; available in PMC 2017 September 14.

Published in final edited form as:

Cell Host Microbe. 2016 September 14; 20(3): 368–380. doi:10.1016/j.chom.2016.07.015.

Single-cell characterization of viral translation-competent reservoirs in HIV-infected individuals

Amy E. Baxter[1,2], **Julia Niessl**[1,2], **Rémi Fromentin**[1], **Jonathan Richard**[1], **Filippos Porichis**[2,3], **Roxanne Charlebois**[1], **Marta Massanella**[1], **Nathalie Brassard**[1], **Nirmin Alsahafi**[1,6], **Gloria-Gabrielle Delgado**[1], **Jean-Pierre Routy**[4], **Bruce D. Walker**[2,3,5], **Andrés Finzi**[1,6], **Nicolas Chomont**[1], and **Daniel E. Kaufmann**[1,2,3,*]

[1]Research Centre of the Centre Hospitalier de l'Université de Montréal (CRCHUM) and Université de Montréal, Montreal, QC H2X 0A9, Canada

[2]Center for HIV/AIDS Vaccine Immunology and Immunogen Discovery (CHAVI-ID), La Jolla, CA 92037, USA

[3]Ragon Institute of Massachusetts General Hospital, Massachusetts Institute of Technology and Harvard University, Cambridge, MA 02139, USA

[4]Chronic Viral Illnesses Service and Division of Hematology, McGill University Health Centre, Montreal, QC H4A 3J1, Canada

[5]Howard Hughes Medical Institute, Chevy Chase, MD 20815, USA

[6]Department of Microbiology and Immunology, McGill University, Montreal, QC H3A 2B4, Canada

SUMMARY

HIV cure efforts are hampered by limited characterization of the cells supporting HIV replication *in vivo* and inadequate methods for quantifying the latent viral reservoir in patients receiving antiretroviral therapy. We combine fluorescent *in situ* RNA hybridization with detection of HIV protein and flow cytometry, enabling detection of 0.5–1 *gag-pol* mRNA+/Gag protein+ infected cells per million. In the peripheral blood of untreated persons, active HIV replication correlated with viremia, and occurred in CD4 T cells expressing T follicular helper cell markers and inhibitory co-receptors. In virally-suppressed subjects, the approach identified latently infected cells capable of producing HIV mRNA and protein after stimulation with PMA/ionomycin and latency-reversing agents (LRAs). While ingenol-induced reactivation mirrored the effector and central/transitional memory CD4 T cell contribution to the pool of integrated HIV DNA, bryostatin-induced reactivation occurred predominantly in cells expressing effector memory

Correspondence: daniel.kaufmann@umontreal.ca.

AUTHOR CONTRIBUTIONS

A.E.B, J.N., F.P, A.F., N.C. and D.E.K. designed the studies; A.E.B., J.N., R.F., J.R., R.C., N.B., G.G.D., M.M, and N.A. performed experiments; J.P.R. obtained IRB approval and recruited participants; B.D.W. provided input on study design; A.E.B. and D.E.K. interpreted the data and wrote the paper with all co-authors' assistance.

The authors have no conflicts of interest to report.

markers. This indicates that CD4 T cell differentiation status differentially affects LRA effectiveness.

eTOC BLURB

Technological limitations hamper characterization of CD4 T cells supporting ongoing HIV infection and quantification of the latent reservoir. Baxter, *et al.* use simultaneous detection of viral protein and mRNA to quantify and phenotype both the ongoing infection during viremia and the translation-competent inducible reservoir in virally-supressed, treated patients.

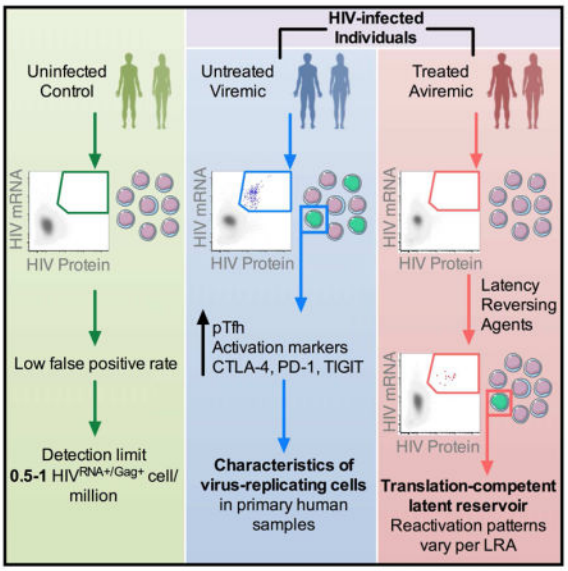

INTRODUCTION

More than three decades after the identification of CD4 T lymphocytes as the main target of human immunodeficiency virus (HIV) infection, surprisingly little is still known about the characteristics of cells that support HIV replication *in vivo* (Swanstrom and Coffin, 2012) and serve as long-lived viral reservoirs in ART-treated individuals (Kulpa and Chomont, 2015). A deeper understanding of the frequency, phenotype and regulation of these cells is critical for the development of targeted HIV cure strategies and vaccines eliciting immune responses capable of eliminating early foci of infection (Burton et al., 2012). Furthermore, determination of the tissue and cellular sources of persistent virus and the development of high-throughput scalable assays to measure the latent reservoir in patients have both been identified as key priorities in HIV eradication research (Deeks et al., 2012). This critical need is demonstrated by the focusing of cure efforts on latency-reversing agents (LRAs) even though their relative ability to induce latently infected cells of different phenotypes and differentiation states is not known.

To accurately measure *in vivo* the frequency and phenotype of CD4 T cells producing viral proteins, we developed a highly sensitive flow cytometry assay enabling simultaneous assessment of HIV RNA and Gag proteins, along with quantitation of phenotypic CD4 T cell molecules. We applied this technology to perform single-cell analysis of CD4 T cells

harboring spontaneously produced and activation-inducible virus in treated and untreated individuals, quantitate viral reservoirs and define the frequency and phenotype of primary CD4 T cells from patient blood that could be induced from latency.

RESULTS

Detection of HIV-infected CD4 T cells by mRNA flow-FISH

Current flow cytometry methods are not sensitive or specific enough to assess HIV-infected cells in patient samples. We thus explored the capacity of fluorescent *in situ* hybridization for gene-specific mRNA (mRNA flow-FISH) to detect HIV transcription in infected CD4 T cells (Porichis et al., 2014). In this approach, multiple oligomeric probes and branched DNA signal amplification enhance detection sensitivity (Figure S1). We selected combined probe sets against the *gag* and *pol* genes as their sequences are well conserved across clinical isolates and they are the most abundant viral transcripts in samples from both treated and untreated patients (Bagnarelli et al., 1996). See Table S1 for sequences used in probe design. Robust mRNA staining was detected in a primary CD4 T cell culture from an HIV-infected individual after expansion of endogenous virus (Figure 1A). Combining this method with staining for HIV protein using the Gag-specific KC57 antibody allowed for concurrent detection of HIV transcription and translation products. We could readily detect double positive ($HIV^{RNA+/Gag+}$) cells in the expanded culture. This population was abrogated by addition of antiviral drugs to the culture and was not present in T cells from uninfected control (UC) donors cultured and processed in parallel (Figure 1B). We define this population of $HIV^{RNA+/Gag+}$ cells as viral translation-competent, as the cells detected contain virus capable of producing HIV mRNA and proteins.

To determine the specificity and linearity of this $HIV^{RNA/Gag}$ assay, we spiked expanded HIV-replicating primary CD4 T cells into uninfected CD4. HIV RNA/protein co-staining showed excellent consistency down to the lowest dilutions tested (23/million, R^2=0.9996, Figures 1CD, 1/million, R^2=0.9856, Figures S2A–B). In contrast, background staining prevented reliable identification of infected cells for frequencies below 0.05–0.1%, the equivalent of 500–1000 HIV^{Gag+} or HIV^{RNA+} T cells per million CD4, when we assessed a single marker (Figures 1EF, S2CD).

To verify that $HIV^{RNA+/Gag+}$ cells were HIV-infected we sorted expanded HIV-infected CD4 T cells into HIV mRNA-negative/Gag protein-negative ($HIV^{neg/neg}$) and $HIV^{RNA+/Gag+}$ populations (Figure S2E) and subsequently measured integrated HIV DNA. The $HIV^{RNA+/Gag+}$ subset was enriched for HIV DNA as compared to the $HIV^{neg/neg}$ population (Figure S2F), confirming that the $HIV^{RNA/Gag}$ assay identifies HIV-infected cells.

We next used confocal microscopy to determine whether this approach could provide semi-quantitative information about viral replication (Figures 1G–I). We expanded primary CD4 T cells isolated from one UC subject and two HIV-infected individuals (one untreated, one ART-treated). We then sorted cell subsets defined by HIV mRNA/protein expression patterns for imaging (Figure 1G, Figures S2G, S3A–C). Spot counting for *gag-pol* mRNA FISH signals revealed a low background in both the UC subject and the $HIV^{neg/neg}$ subset and clear signals in the three HIV^{RNA+} populations (Figure 1H, Figure S2H). Based on the false

positive rate observed in the UC patient (Figure S2H), we determined a conservative detection limit to minimize false-positive events (assuming Gaussian distribution, mean +3SD) of 20 gag-pol mRNA spots per cell. This accounts for 93% of all HIV^{RNA+} cells (Figure S2H). The hierarchy of total *gag-pol* mRNA spot counts was consistent with flow cytometry MFIs of the sorted populations, with the $HIV^{RNA\,bright/Gag\,bright}$ cells harboring most spots (Figure 1H). As the intensity of individual spots will contribute to the global signal intensity of a given cell, we examined the total intensity of *gag-pol* mRNA signal for individual cells using corrected total cell fluorescence (CTCF) (Burgess et al., 2010). Again, we found a direct relationship to flow cytometry data (Figures S3D–H).

We measured the relative distribution of *gag-pol* RNA spots in the nuclear and cytoplasmic compartments amongst the sorted subsets. In $HIV^{RNA+/Gag-}$ cells, the vast majority of the *gag-pol* RNA spots were located in the nucleus and only a small fraction (median 5.1%) in the cytoplasm, whereas this proportion reached 30–40% in subsets also expressing Gag protein (Figure 1I). Such differences in localization were confirmed by Z-stack imaging (Movies S1–2). This is consistent with data suggesting that viral transcription leads to accumulation of *gag-pol* mRNA in the nucleus before its egress to the cytoplasm is enabled by Rev-mediated export (Karn and Stoltzfus, 2012). Although this assay is not designed for single molecule FISH, we demonstrate that it can be used semi-quantitatively to assess HIV transcription at the single-cell level. When used sequentially in flow sorting and confocal microscopy, it can greatly facilitate FISH studies of rare cell subsets of interest in heterogeneous populations.

Frequencies of HIV-producing CD4 T cells in the blood of untreated patients

Having validated the assay on infected CD4 T cells expanded *in vitro,* we next sought to determine the frequency of cells that produce HIV at a given time in the peripheral blood of subjects with untreated HIV infection (UNT), compared to UC donors (subject characteristics and number of cells analyzed: Table S2). We quantified in parallel the population that spontaneously produces viral mRNA and proteins and the additional cells that can be induced to express such viral markers after short-term 12 hr PMA/ionomycin (PMA/iono) stimulation. Whereas false positive events were very rare in UC (one $HIV^{RNA+/Gag+}$ cell detected from 8 samples/7.7 million cells), we readily detected $HIV^{RNA+/Gag+}$ CD4 in UNT subjects (median[range]=123[1.5–230]/per million CD4) (Figures 2AB), which were further increased upon stimulation with PMA/iono (median[range]=311[3.6–768]/million). The impact of PMA/iono was similar amongst subjects (Figure 2C, Figure S4A). This suggested that, besides CD4 T cells spontaneously producing viral proteins, an additional larger pool of infected lymphocytes appeared poised for rapid induction of viral transcription and translation upon stimulation in UNT individuals. The superiority of the RNA/protein co-staining method over single marker use was clear when we compared unstimulated, primary samples of UC to UNT donors (Figure 2D). The limit of $HIV^{RNA+/Gag+}$ cell detection based on the UC false positive detection rate was 0.5–1/million, whereas high background staining rendered single KC57 Gag or mRNA staining alone non-interpretable in the 0–1000 cells/million range, the frequency bracket that contained all UNT subjects examined. This represents a gain in detection of 1000-fold over standard protein staining for HIV Gag.

We next assessed the correlation of $HIV^{RNA+/Gag+}$ frequencies with markers of disease progression. There was a strong correlation with viral load in both the resting and PMA/iono stimulated conditions (Figure 2E, Figure S4C) and non-significant inverse correlations with CD4 count (Figure 2F, Figure S4B). Interestingly, we found the strongest correlations between the absolute number of HIV-infected cells per μL and viral load (Figure 2G). We also observed an increase in the *gag-pol* mRNA and Gag protein MFI on $HIV^{RNA+/Gag+}$ cells following stimulation, suggesting increased viral production per cell when compared to spontaneous viral production (Figure S4DE). We confirmed the reproducibility of the assay across different experiments, flow panels and operators, even at lower frequencies of $HIV^{RNA+/Gag+}$ CD4 (Figure S4F). Therefore, CD4 T cells that produce HIV RNAs and protein, either spontaneously *ex vivo* or after stimulation, can be reliably identified and quantified in primary clinical samples from subjects with progressive HIV infection.

HIV-infected CD4 T cells preferentially express a central/transitional memory phenotype

The features of cells harboring replicating virus have thus far been largely inferred from *in vitro* infection or amplification of autologous virus, due to an inability to detect infected cells *ex vivo* using previously applied methods. To address this, we assessed the phenotype of $HIV^{RNA+/Gag+}$ CD4 T cells in primary UNT samples, analyzed directly from leukapheresis donation and without additional *ex vivo* stimulation. Such cells are defined here as *in vivo* infected. CD4 down-regulation is a hallmark of HIV infection *in vitro,* facilitating Env incorporation and viral replication (Arganaraz et al., 2003). We found that CD4 expression was profoundly diminished on *in vivo* infected $HIV^{RNA+/Gag+}$ cells (Figures 3A–C), consistent with previous data (DeMaster et al., 2015). HLA-Class I downregulation, another well-known effect of Nef protein (Schwartz et al., 1996) was also observed in primary samples (Figure 3D), albeit at a more modest level than after stimulation and virus propagation *ex vivo* (Figure 3E). In contrast, HLA-Class II expression on *in vivo* infected cells differed from *in vitro* data; consistent with an activated state, HLA-DR was preferentially expressed on $HIV^{RNA+/Gag+}$ compared to $HIV^{RNA-/Gag-}$ cells in primary samples (Figure 3F), whereas no enrichment for HIV-infected cells in the HLA-DR+ population was observed at days 5 and 7 of endogenous viral reactivation (Figure 3G). Differences were also observed for PD-L1 expression on $HIV^{RNA+/Gag+}$ (Figures S5AB). Whereas PD-L1 was highly expressed on stimulated HIV-infected and non-infected cells early after initiation (e.g., day 3) of T cell cultures, suggesting a potential mechanism of functional immune escape similar to that described for cancer cells, PD-L1 expression was low on *in vivo* infected $HIV^{RNA+/Gag+}$ CD4. The latter was surprising given the same cells preferentially expressed HLA-DR, another marker of activation. Thus, the phenotype of HIV-replicating cells *in vivo* cannot be reliably inferred from *in vitro* expansion models.

Central memory cells are major long-lived viral reservoirs in ART-treated subjects (Chomont et al., 2009). However, whether viral replication during viremia preferentially occurs in this subset remains to be defined. We analyzed the differentiation of $HIV^{RNA+/Gag+}$ CD4 T cells according to CD45RA and CD27 expression (Figure 3H), described here as naive (T_{naive}: $CD27^+$ $CD45RA^+$), central/transitional memory ($T_{CM/TM}$: $CD27^+$ $CD45RA^-$), effector memory (T_{EM}: $CD27^-$ $CD45RA^-$) and terminally differentiated (T_{TD}: $CD27^-$ $CD45RA^+$) cells (Sallusto et al., 2004). The $T_{CM/TM}$ phenotype was dominant amongst $HIV^{RNA+/Gag+}$

cells (median[range]=40.90%[31.5–60], normalized mean=53.4%), in keeping with observations made for HIV DNA content in ART-treated patients (Figures 3I, S5CD, S6G). Compared to the $HIV^{neg/neg}$ population, HIV-infected cells contained few T_{naive} or T_{TD} CD4 and were enriched in both $T_{CM/TM}$ and T_{EM}. Thus, HIV-infected cells do not appear to shift towards a more differentiated phenotype in UNT individuals, in spite of high activation.

HIV-infected cells in blood preferentially express T follicular helper cell markers and inhibitory co-receptors

Germinal center Tfh are critical for B cell help. Studies using viral outgrowth assays (VOA; (Finzi et al., 1997)) and/or PCR quantitation have shown that Tfh serve as preferential sites of viral replication in lymph nodes in the absence of therapy (Perreau et al., 2013), and may represent a viral reservoir in controlled viremia (Banga et al., 2016). A peripheral blood equivalent of Tfh (pTfh) corresponding to a memory population has recently been identified (Morita et al., 2011) and predicts development of broadly neutralizing antibodies against HIV (Locci et al., 2013). We thus sought to define whether pTfh are preferentially infected. Indeed, pTfh, defined as $CD45RA^{-}$ memory CD4 T cells co-expressing PD-1 and CXCR5, were enriched in $HIV^{RNA+/Gag+}$ cells (Figures 4AB). Expression of ICOS, a critical co-stimulator for Tfh function, was also highly enriched in $HIV^{RNA+/Gag+}$, suggesting recent activation (Figure 4C). However, there was no significant difference in expression of CXCR3, a classical Th1 marker whose co-expression identifies a less functional subset of Tfh but can also be induced by activation (Figure S5E). Thus, preferential replication of HIV in activated Tfh cells is not restricted to germinal centers but can also be detected in the periphery.

Blockade of inhibitory co-receptors of TCR signaling is considered a potential means of viral reactivation in “shock and kill” strategies (Deeks, 2012). Besides mediating CD4 T cell exhaustion (Kaufmann et al., 2007), molecules such as PD-1 may contribute to the maintenance of the quiescent state of viral latency in HIV-infected CD4 T cells; the $PD\text{-}1^{+}$ subset is a preferential viral reservoir in ART-treated subjects (Chomont et al., 2009). Expression of multiple inhibitory receptors on CD4 T cells prior to ART was shown to be a predictive biomarker of viral rebound post treatment interruption, suggesting that they may identify those latently infected cells with a higher proclivity to viral transcription (Hurst et al., 2015). However, this link between inhibitory co-receptor expression and spontaneous production of viral mRNA and protein has not been demonstrated in untreated infection. We therefore determined the expression patterns of the receptors PD-1, CTLA-4 and TIGIT on HIV-infected cells, molecules that are all either already targeted by cancer immunotherapies in clinical care or the subject of active drug development (Figures 4D–F, Figures S5F-H). Analysis of individual receptors showed that the $PD\text{-}1^{+}$, $TIGIT^{+}$ and $CTLA\text{-}4^{+}$ populations were all enriched for $HIV^{RNA+/Gag+}$ T cells. Indeed, the majority (median=70%) of $HIV^{RNA+/Gag+}$ CD4 T cells expressed at least one inhibitory receptor, while even in UNT patients a minority of the uninfected, $HIV^{neg/neg}$ CD4 T cells (median=35%) expressed such exhaustion markers (Figures 4GH). The majority of $HIV^{RNA+/Gag+}$ CD4 T cells expressed PD-1 (median = 63%), in agreement with observations made on HIV DNA content in ART-treated patients, whereas a somewhat smaller fraction expressed TIGIT (median=42%). By analyzing patterns of inhibitory receptor coexpression, we observed that half of the $PD\text{-}1^{+}$

cells also expressed TIGIT, while $TIGIT^+$ only cells were less frequent. The same trends were observed for $HIV^{neg/neg}$ CD4. While the frequency of CTLA-4^+ T cells was the lowest for the coreceptors studied, the relative enrichment of $HIV^{RNA+/Gag+}$ T cells compared to uninfected T cells was greatest for these populations. In particular, while PD-1^+ CTLA-4^+ and the triple positive (CTLA-4^+ PD-1^+ $TIGIT^+$) populations represented small subsets (<1%) in the uninfected T cell population, both of these populations were detectable at higher frequencies (~4%) in the $HIV^{RNA+/Gag+}$ infected T cells. These data show that robust viral replication occurs in blood lymphocytes in spite of high levels of inhibitory receptor co-expression.

Quantitation of latent reservoirs from virally suppressed individuals and correlation with PCR-based assays

Strategies to reduce the latent reservoirs are now being tested in clinical trials (Archin et al., 2012). There is an urgent need for high-throughput assays able to reliably quantify these cells in subjects, but their low frequency makes this challenging. Furthermore, estimation of reservoir size varies widely depending on the assay used (Eriksson et al., 2013), with the VOA giving a minimal value for the replication-competent reservoir and DNA PCR-based assays overestimating its size due to defective viral genomes. Here, we examined ART-treated subjects (Tx, characteristics and cells analyzed, Table S3) to assess the ability of the $HIV^{RNA/Gag}$ assay to quantify latently infected CD4 T cells harboring inducible virus capable of translating Gag and compared it to alternative measurements of reservoir size. As previously, we define this population as the viral translation-competent latent reservoir. In the absence of stimulation, $HIV^{RNA+/Gag+}$ events were very rare or absent (median[range]=0.55[0–2.6], Figures 5AB), in keeping with published data utilizing HIV Gag protein staining alone, where rare HIV^{Gag+} cells were detected in ART-treated patients (Graf et al., 2013). In contrast, PMA/iono stimulation induced $HIV^{RNA+/Gag+}$ cells in all but one Tx subject, with frequencies ranging from 1.2 to 660/million (median=3.56, Figures 5AB, Figure S6C). Reactivation of the translation-competent latent reservoir measured by our assay showed a strong trend (p=0.061) towards inverse correlation with CD4/CD8 ratio (Figure 5C) and a weaker inverse correlation with CD4 T cell count (Figure S6A). We next compared the frequency of $HIV^{RNA+/Gag+}$ events to the estimated size of the reservoir based on integrated or total HIV DNA (Figure 5D). While the size of the reservoir determined by these assays correlated well (Figure 5E, Figure S6B), the median reservoir size as measured by integrated DNA was ~800 copies/million compared to 3.56 cells/million by the $HIV^{RNA/Gag}$ assay. The median ratio between these two measures was 204, which is comparable to the differences detected between integrated DNA and the VOA (Bruner et al., 2015). Factors that may contribute to these differences include the inability of standard DNA assays to distinguish between replication-competent and defective integrated viral genomes (while the $HIV^{RNA/Gag}$ assay detects only cells infected with virus capable of producing viral RNA and protein, thus narrowing estimates of the functional reservoir) and the possibility of multiple integration events in a cell. In addition, the stimulus used may play a role, as not all competent virus may be reactivated by a single round of potent stimulation (Ho et al., 2013) and detection of reactivated virus is limited to those proviruses able to produce Gag protein within the time frame of the assay.

We then compared the $HIV^{RNA/Gag}$ assay to the VOA in a subset of 11 patients (Figure S6DE, Table S4). The $HIV^{RNA/Gag}$ assay and VOA detected a median[range] of 4.65[0–110.4] $HIV^{RNA+/Gag+}$ translation-competent and 1.43[0.06–32.23] replication-competent HIV-infected cells/million CD4 respectively. In comparison, the median int.DNA copies/million CD4 for these patients was 648. Thus, while the relative frequencies measured by the VOA and $HIV^{RNA/Gag}$ assay varied and did not correlate in this group of patients, they were much closer in magnitude than the PCR-based measure.

We next tested the ability of the protein kinase C modulators bryostatin, an antineoplastic drug currently in clinical cancer trials, and ingenol, currently approved to topically treat actinic keratosis, to induce production of viral mRNA and proteins. Bryostatin, ingenol and their analogues have potent HIV LRA activity *in vitro* (DeChristopher et al., 2012; Jiang et al., 2014). We detected HIV reactivation in all Tx and UNT subjects examined although at varying degrees (Figure 6ABC). In the majority of Tx patients, induction of the reservoir by both LRAs bryostatin (median[range]=1.2[0.91–37.9]) and ingenol (median[range]=1.38[1.01–3.36]) was lower than that of PMA/iono (median[range]=7.5[0.86–660]). However response to all stimuli varied considerably between donors. In contrast, in UNT subjects the response to bryostatin was close (68–79%) to that of PMA/iono, likely reflecting the major difference in regulation of HIV gene expression in these two contexts. Finally, we examined the phenotype of latently infected cells reactivated with bryostatin and ingenol, as surface markers are much better preserved with these LRAs than with PMA/iono treatment.

In UNT patients, HIV-infected CD4 were predominantly T_{CM}/T_{TM} and T_{EM} in both ongoing and bryostatin-reactivated infection (Figure 6DE). Concordantly, integrated HIV DNA was localized to these compartments (Figure S6F). Though the number of $HIV^{RNA+/Gag+}$ CD4 more than doubled (Figure 6C) following bryostatin reactivation, the proportion of HIV-infected T_{CM}/T_{TM} compared to T_{EM} was not significantly changed (Figure 6E). This suggests that, in individuals with ongoing viremia, bryostatin is able to reactivate a viral translation-competent reservoir from both the $T_{CM/TM}$ and T_{EM} compartments.

In comparison, in Tx subjects, the majority of bryostatin-reactivated $HIV^{RNA+/Gag+}$ cells were T_{EM} (Figures 6FG), with T_{CM} contributing a minority fraction to the reactivated population. Indeed, over 90% of bryostatin-reactivated $HIV^{RNA+Gag+}$ cells were detected in the $T_{EM.}$ In contrast, in a subset of the same patients, ingenol reactivated $HIV^{RNA+/Gag+}$ cells from both T_{CM}/T_{TM} and T_{EM} in proportions comparable to those in the $HIV^{neg/neg}$ population (Figure 6HI). Interestingly, when the frequency of cells harboring integrated HIV DNA was assessed, both T_{CM}/T_{TM} and T_{EM} contributed to the persistent reservoir (Figures S6GH). Therefore, despite the presence of integrated DNA in both memory subsets, bryostatin-induced reactivation as measured with the $HIV^{RNA/Gag}$ assay was mostly limited to the T_{EM} compartment, while ingenol-induced reactivation was not. This suggests that the differentiation status of CD4 T cells may not affect all LRAs equally, even those from the same class.

DISCUSSION

Here, we establish and validate a flow-based RNA FISH assay to assess ongoing viral replication and the size of the inducible latent reservoir in HIV-infected individuals, and additionally demonstrate its ability to determine the efficacy of LRAs and the phenotype of the induced latently infected cells. The accurate detection of cells harboring virus able to produce HIV RNA and protein down to frequencies of 0.5–1/million CD4 T cells, combined with the power of single-cell analysis by polychromatic flow cytometry, enabled quantitative and phenotypic characterization of HIV-infected cells directly sampled from patient blood. While previous reports have utilized FISH-based techniques to identify HIV-infected cells (Patterson et al., 2001), the use of concurrent protein staining to identify the translation-competent reservoir allows increased specificity. Our data pinpoint markers of CD4 T cells supporting HIV replication in progressive disease, including features that cannot easily be inferred from *in vitro* infection, such as enrichment in the pTfh compartment and in the HLA-DR+ subset. Consistent with published data using integrated DNA as a measure of infection (Brenchley et al., 2004) we observe the localization of HIV-infected CD4 in the memory compartment, with limited infection of naïve CD4. We also show that HIV-infected cells are more likely to express markers of exhaustion (PD-1, CTLA-4 and TIGIT) than uninfected CD4 in the context of ongoing viremia. The role for exhaustion markers in the context of CD4 infection remains to be determined – for example, are cells expressing such markers more likely to be infected *in vivo*, or is expression a consequence of infection itself. As multiple exhaustion markers (including PD-1) are also upregulated as negative feedback mechanisms following activation, an increased susceptibility of these cells to infection is in line with the observations made here and previously (Stevenson et al., 1990) that activated cells are more amenable to HIV infection. In the context of latency, it has been suggested that the expression of multiple inhibitory receptors may identify those CD4 with a higher proclivity to viral transcription (Hurst et al., 2015). The work presented here focuses on CD4 T cells as the major source of infectious virus during chronic infection and the major reservoir in patients receiving therapy. However additional cell types have been reported as permissive to HIV in vivo, including macrophages and dendritic cells. Previous work has demonstrated that monocytes can be assessed (Porichis et al., 2014), thus these subsets could be evaluated by applying the $HIV^{RNA/Gag}$ technique to tissues.

We also narrow down estimates for the size of the inducible reservoir (median 3.56 cell/million CD4 following 12 hr PMA/ionomycin activation, median 204-fold lower than integrated DNA) while demonstrating wide differences amongst subjects with suppressed viral load on therapy. When compared with alternative measurements of reservoir size, the $HIV^{RNA/Gag}$ assay most closely mirrors findings using the VOA, where the minimum size of the replication-competent reservoir is estimated to be 1 per million resting CD4 (1.4 in our cohort), 100–1000 fold less than that measured by integrated DNA. In addition, both the reservoir size as measured by the $HIV^{RNA/Gag}$ assay here and the VOA, shown previously (Kiselinova et al., 2016), correlate with the reservoir measured by integrated HIV DNA. The advantage of the $HIV^{RNA/Gag}$ assay is the direct detection of HIV-infected cells, allowing phenotyping, which is not possible with the VOA. Both assays have the limitation that they may not detect all intact proviruses, due to the stochastic nature of reactivation and the

stimuli used. Furthermore, while the VOA detects replication-competent virus (defined by the ability of secreted virus to establish a spreading infection *in vitro*), the $HIV^{RNA/Gag}$ assay detects cells containing virus able to produce HIV RNA and Gag protein (viral translation-competent virus). Therefore one potential caveat for the $HIV^{RNA/Gag}$ assay is that not all of the reactivated virus is infectious and so the size of the replication-competent reservoir may be slightly overestimated. In contrast, the VOA may underestimate the size of the replication-competent reservoir as virus may be released, but may not establish an in vitro infection and remain undetectable. These differences may explain the lack of correlation observed between these two assays and the larger reservoir size detected using the $HIV^{RNA/Gag}$ assay when compared to the VOA.

An additional factor in the detection of rare cells is the probability of detecting events due to Poisson distribution and sampling differences. To increase the probability of accurately detecting rare cells, increasing cell numbers must be analyzed. In the current study, 2–3 million CD4 T cells per patient per condition were usually acquired on the flow cytometer. The requirement for high cell numbers may be a limiting factor for latency studies; however, a similar restriction exists for known techniques to measure latent reservoirs.

Finally, we show that this approach can be used to assess the efficiency of LRAs such as bryostatin and ingenol, drugs currently in clinical trials, and importantly determine the susceptibility of distinct CD4 cells to LRA-induced reactivation. The need for such primary cell assays is highlighted by the wide variability of results obtained in *in vitro* latency models (Spina et al., 2013). The phenotypic analysis of LRA-induced cells has important potential implications for the function of LRAs. Firstly, while both the T_{EM} and T_{CM} CD4 pools contain integrated pro-virus, the relative frequencies of functional versus defective pro-viral DNA have been suggested to differ between subsets (Soriano-Sarabia et al., 2014). Alternatively, CD4 subsets may vary in their sensitivity to individual LRAs. While these two mechanisms are not mutually exclusive, our data suggest a differential sensitivity of CD4 populations to individual LRAs: bryostatin readily induced the T_{EM} reservoir, but had limited effect on the T_{CM} compartment, contrasting with the more even effect observed with ingenol. An effective LRA must induce HIV protein expression in all latently infected cells regardless of phenotype to enable recognition and elimination by host immune responses, and as such ingenol may represent a promising candidate. Combinations of LRAs need to be assessed, to increase potency but also to recruit additional subsets of latently infected cells that may not be amenable to reactivation with a single drug. This technology and the results obtained may have important implications for HIV pathogenesis studies, including investigation of early transmission events, testing of LRAs and monitoring of cure strategies.

EXPERIMENTAL PROCEDURES

Participants and Samples

Leukaphereses were obtained from study participants at the Montreal General Hospital, Montreal, Canada and at Martin Memorial Health Systems, Florida, USA. The study was approved by the respective IRBs and written informed consent obtained from all participants prior to enrolment. See Supplemental Experimental Procedures for details. Untreated, viremic participants (UNT) were either treatment naïve, or untreated for at least 6 months.

Treated subjects (Tx) were on ART for over 12 months with controlled viral load (<50 vRNA copies/mL) for at least 6 months. Patient characteristics are summarized in Tables S2–S4. In rare cases, due to limited sample availability, sequential leukaphereses were used for individual subjects. PBMC isolated by Ficoll density gradient were stored in liquid nitrogen.

In vitro reactivation and spreading infection

CD4 T cells were isolated from PBMC by negative magnetic bead selection (StemCell), resulting in an untouched population defined as CD3+CD4+/-CD8-CD14-CD19- (purity routinely over 95%). Cells were stimulated for 36–40 hr in RPMI with PHA-L (10μg/ml, Sigma) and IL-2 (50U/ml), then washed and maintained for 6–7 days in RPMI with IL-2 (100U/ml). In some experiments, ARVs (T20 (7.5μg/ml) + AZT (1μM)) were added. Enfuvirtide (T-20), Zidovudine (AZT), and IL-2 (Lahm and Stein, 1985) were obtained through NIH AIDS Reagent Program, Division of AIDS, NIAID, NIH: human rIL-2 from Dr. Maurice Gately, Hoffmann - La Roche Inc.

Reactivation of latent infection with PMA/ionomycin or LRAs

CD4 T cells were isolated as above, resuspended at 2×10^6/ml media with ARVs (T20 + AZT, as before) and rested for 3–5 hr. Cells were either unstimulated, stimulated for 12 hr with PMA (50ng/ml) and ionomycin (0.5μg/ml), or for 18 hr with Bryostatin-1 (10nM, Enzo Life Sciences) or Ingenol-3-angelate (25nM, Sigma). $5–12 \times 10^6$ purified CD4 were required per patient/condition.

$HIV^{RNA/Gag}$ Assay

See Figure S1 for the workflow schematic. Samples were subjected to the PrimeFlow RNA assay (Affymetrix/eBioscience) as per manufacturer's instructions. See Supplemental Experimental Procedures for protocol details and antibody panels. Cells were stained for viability, surface stained for phenotypic markers and stained intracellulary for HIV Gag protein prior to mRNA detection. Samples were acquired on an LSRII (BD Bioscience). Analysis was performed using FlowJo (Treestar, V10).

Linearity and specificity experiment

Reactivated, HIV-replicating CD4 T cells from an untreated patient were spiked into uninfected cells at different ratios to set up a dilution series. The predicted frequency of $HIV^{RNA+/Gag+}$ (or HIV^{RNA+} or HIV^{Gag+}) was compared to the detected frequency. See Supplemental Experimental Procedures for details.

Microscopy on sorted CD4 following $HIV^{RNA+/Gag+}$ Assay

Patient reactivated CD4 T cells were sorted according to expression of Gag protein and GagPol mRNA. The number of nuclear and total *gag-pol* mRNA spots and CTCF was determined by confocal microscopy. See Supplemental Experimental Procedures for details.

HIV DNA quantification

Quantifications of total and integrated HIV DNA were determined as previously described (Vandergeeten et al., 2014).

QVOA

Quantifications of replication-competent virus were performed as previously described (Siliciano and Siliciano, 2005).

Statistics

All statistical analyses were performed in Prism (V6, GraphPad). Data was tested for normality using the D'Augustino-Pearson Omnibus normality test. Where appropriate, parametric tests were applied. Statistical tests were two-sided and repeated measures used for comparisons within subjects. For comparisons between groups, Kruskal-Wallis or Friedman one-way ANOVA with Dunn's post-test was used. For correlations, Spearman's R (R^S) correlation coefficient was used. For pair-wise analysis of non-normally distributed data, Wilcoxon Signed Rank t-tests were used. $P<0.05$ were considered significant.

Supplementary Material

Refer to Web version on PubMed Central for supplementary material.

Acknowledgments

We thank Josée Girouard, the clinical staff at McGill University Health Centre and all study participants; Drs Dominique Gauchat and the CRCHUM Flow Cytometry Platform, Daniel Zenklusen and Chunfai Lai for technical assistance; Dylan Malayter for reagents and Drs Shane Crotty and Naglaa Shoukry for their input on this manuscript.

This study was supported by the National Institutes of Health (HL-092565, AI100663 CHAVI-ID, AI113096, AI118544 and the Delaney AIDS Research Enterprise (DARE) 1U19AI096109); the Canadian Institutes for Health Research (grant #137694; Canadian HIV Cure Enterprise), a Canada Foundation for Innovation grant, the FRQS AIDS and Infectious Diseases Network and the Foundation for AIDS Research (108928-56-RGRL). D.E.K and N.C. are supported by FRQS Research Scholar Awards. A.F. is the recipient of a Canada Research Chair. J.P.R is the holder of Louis Lowenstein Chair, McGill University. J.R. is the recipient of a CIHR Fellowship Award #135349. N.A. is the recipient of a King Abdullah scholarship from the Saudi Government.

References

Archin NM, Liberty AL, Kashuba AD, Choudhary SK, Kuruc JD, Crooks AM, Parker DC, Anderson EM, Kearney MF, Strain MC, et al. Administration of vorinostat disrupts HIV-1 latency in patients on antiretroviral therapy. Nature. 2012; 487:482–485. [PubMed: 22837004]

Arganaraz ER, Schindler M, Kirchhoff F, Cortes MJ, Lama J. Enhanced CD4 down-modulation by late stage HIV-1 nef alleles is associated with increased Env incorporation and viral replication. J Biol Chem. 2003; 278:33912–33919. [PubMed: 12816953]

Bagnarelli P, Valenza A, Menzo S, Sampaolesi R, Varaldo PE, Butini L, Montroni M, Perno CF, Aquaro S, Mathez D, et al. Dynamics and modulation of human immunodeficiency virus type 1 transcripts in vitro and in vivo. J Virol. 1996; 70:7603–7613. [PubMed: 8892880]

Banga R, Procopio FA, Noto A, Pollakis G, Cavassini M, Ohmiti K, Corpataux JM, de Leval L, Pantaleo G, Perreau M. PD-1 and follicular helper T cells are responsible for persistent HIV-1 transcription in treated aviremic individuals. Nat Med. 2016

Brenchley JM, Hill BJ, Ambrozak DR, Price DA, Guenaga FJ, Casazza JP, Kuruppu J, Yazdani J, Migueles SA, Connors M, et al. T-cell subsets that harbor human immunodeficiency virus (HIV) in vivo: implications for HIV pathogenesis. J Virol. 2004; 78:1160–1168. [PubMed: 14722271]

Bruner KM, Hosmane NN, Siliciano RF. Towards an HIV-1 cure: measuring the latent reservoir. Trends Microbiol. 2015; 23:192–203. [PubMed: 25747663]

Burgess A, Vigneron S, Brioudes E, Labbe JC, Lorca T, Castro A. Loss of human Greatwall results in G2 arrest and multiple mitotic defects due to deregulation of the cyclin B-Cdc2/PP2A balance. Proc Natl Acad Sci U S A. 2010; 107:12564–12569. [PubMed: 20538976]

Burton DR, Ahmed R, Barouch DH, Butera ST, Crotty S, Godzik A, Kaufmann DE, McElrath MJ, Nussenzweig MC, Pulendran B, et al. A Blueprint for HIV Vaccine Discovery. Cell Host Microbe. 2012; 12:396–407. [PubMed: 23084910]

Chomont N, El-Far M, Ancuta P, Trautmann L, Procopio FA, Yassine-Diab B, Boucher G, Boulassel MR, Ghattas G, Brenchley JM, et al. HIV reservoir size and persistence are driven by T cell survival and homeostatic proliferation. Nat Med. 2009; 15:893–900. [PubMed: 19543283]

DeChristopher BA, Loy BA, Marsden MD, Schrier AJ, Zack JA, Wender PA. Designed, synthetically accessible bryostatin analogues potently induce activation of latent HIV reservoirs in vitro. Nat Chem. 2012; 4:705–710. [PubMed: 22914190]

Deeks SG. HIV: Shock and kill. Nature. 2012; 487:439–440. [PubMed: 22836995]

Deeks SG, Deeks SG, Autran B, Berkhout B, Benkirane M, Cairns S, Chomont N, Chun TW, Churchill M, Di Mascio M, et al. Towards an HIV cure: a global scientific strategy. Nat Rev Immunol. 2012; 12:607–614. [PubMed: 22814509]

DeMaster LK, Liu X, VanBelzen DJ, Trinite B, Zheng L, Agosto LM, Migueles SA, Connors M, Sambucetti L, Levy DN, et al. A Subset of CD4/CD8 Double-Negative T Cells Expresses HIV Proteins in Patients on Antiretroviral Therapy. J Virol. 2015; 90:2165–2179. [PubMed: 26537682]

Eriksson S, Graf EH, Dahl V, Strain MC, Yukl SA, Lysenko ES, Bosch RJ, Lai J, Chioma S, Emad F, et al. Comparative analysis of measures of viral reservoirs in HIV-1 eradication studies. PLoS Pathog. 2013; 9:e1003174. [PubMed: 23459007]

Finzi D, Hermankova M, Pierson T, Carruth LM, Buck C, Chaisson RE, Quinn TC, Chadwick K, Margolick J, Brookmeyer R, et al. Identification of a reservoir for HIV-1 in patients on highly active antiretroviral therapy. Science. 1997; 278:1295–1300. [PubMed: 9360927]

Graf EH, Pace MJ, Peterson BA, Lynch LJ, Chukwulebe SB, Mexas AM, Shaheen F, Martin JN, Deeks SG, Connors M, et al. Gag-positive reservoir cells are susceptible to HIV-specific cytotoxic T lymphocyte mediated clearance in vitro and can be detected in vivo [corrected]. PLoS One. 2013; 8:e71879. [PubMed: 23951263]

Ho YC, Shan L, Hosmane NN, Wang J, Laskey SB, Rosenbloom DI, Lai J, Blankson JN, Siliciano JD, Siliciano RF. Replication-competent noninduced proviruses in the latent reservoir increase barrier to HIV-1 cure. Cell. 2013; 155:540–551. [PubMed: 24243014]

Hurst J, Hoffmann M, Pace M, Williams JP, Thornhill J, Hamlyn E, Meyerowitz J, Willberg C, Koelsch KK, Robinson N, et al. Immunological biomarkers predict HIV-1 viral rebound after treatment interruption. Nat Commun. 2015; 6:8495. [PubMed: 26449164]

Jiang G, Mendes EA, Kaiser P, Sankaran-Walters S, Tang Y, Weber MG, Melcher GP, Thompson GR 3rd, Tanuri A, Pianowski LF, et al. Reactivation of HIV latency by a newly modified Ingenol derivative via protein kinase Cdelta-NF-kappaB signaling. AIDS. 2014; 28:1555–1566. [PubMed: 24804860]

Karn J, Stoltzfus CM. Transcriptional and posttranscriptional regulation of HIV-1 gene expression. Cold Spring Harb Perspect Med. 2012; 2:a006916. [PubMed: 22355797]

Kaufmann DE, Kavanagh DG, Pereyra F, Zaunders JJ, Mackey EW, Miura T, Palmer S, Brockman M, Rathod A, Piechocka-Trocha A, et al. Upregulation of CTLA-4 by HIV-specific CD4+ T cells correlates with disease progression and defines a reversible immune dysfunction. Nature immunology. 2007; 8:1246–1254. [PubMed: 17906628]

Kiselinova M, De Spiegelaere W, Buzon MJ, Malatinkova E, Lichterfeld M, Vandekerckhove L. Integrated and Total HIV-1 DNA Predict Ex Vivo Viral Outgrowth. PLoS Pathog. 2016; 12:e1005472. [PubMed: 26938995]

Kulpa DA, Chomont N. HIV persistence in the setting of antiretroviral therapy: when, where and how does HIV hide? J Virus Erad. 2015; 1:59–66. [PubMed: 26448966]

Lahm HW, Stein S. Characterization of recombinant human interleukin-2 with micromethods. J Chromatogr. 1985; 326:357–361. [PubMed: 3875623]

Locci M, Havenar-Daughton C, Landais E, Wu J, Kroenke MA, Arlehamn CL, Su LF, Cubas R, Davis MM, Sette A, et al. Human circulating PD-(+)1CXCR3(-)CXCR5(+) memory Tfh cells are highly functional and correlate with broadly neutralizing HIV antibody responses. Immunity. 2013; 39:758–769. [PubMed: 24035365]

Morita R, Schmitt N, Bentebibel SE, Ranganathan R, Bourdery L, Zurawski G, Foucat E, Dullaers M, Oh S, Sabzghabaei N, et al. Human blood CXCR5(+)CD4(+) T cells are counterparts of T follicular cells and contain specific subsets that differentially support antibody secretion. Immunity. 2011; 34:108–121. [PubMed: 21215658]

Patterson BK, McCallister S, Schutz M, Siegel JN, Shults K, Flener Z, Landay A. Persistence of intracellular HIV-1 mRNA correlates with HIV-1-specific immune responses in infected subjects on stable HAART. Aids. 2001; 15:1635–1641. [PubMed: 11546937]

Perreau M, Savoye AL, De Crignis E, Corpataux JM, Cubas R, Haddad EK, De Leval L, Graziosi C, Pantaleo G. Follicular helper T cells serve as the major CD4 T cell compartment for HIV-1 infection, replication, and production. The Journal of experimental medicine. 2013; 210:143–156. [PubMed: 23254284]

Porichis F, Hart MG, Griesbeck M, Everett HL, Hassan M, Baxter AE, Lindqvist M, Miller SM, Soghoian DZ, Kavanagh DG, et al. High-throughput detection of miRNAs and gene-specific mRNA at the single-cell level by flow cytometry. Nat Commun. 2014; 5:5641. [PubMed: 25472703]

Sallusto F, Geginat J, Lanzavecchia A. Central memory and effector memory T cell subsets: function, generation, and maintenance. Annu Rev Immunol. 2004; 22:745–763. [PubMed: 15032595]

Schwartz O, Marechal V, Le Gall S, Lemonnier F, Heard JM. Endocytosis of major histocompatibility complex class I molecules is induced by the HIV-1 Nef protein. Nat Med. 1996; 2:338–342. [PubMed: 8612235]

Siliciano JD, Siliciano RF. Enhanced culture assay for detection and quantitation of latently infected, resting CD4+ T-cells carrying replication-competent virus in HIV-1-infected individuals. Methods Mol Biol. 2005; 304:3–15. [PubMed: 16061962]

Soriano-Sarabia N, Bateson RE, Dahl NP, Crooks AM, Kuruc JD, Margolis DM, Archin NM. Quantitation of replication-competent HIV-1 in populations of resting CD4+ T cells. J Virol. 2014; 88:14070–14077. [PubMed: 25253353]

Spina CA, Anderson J, Archin NM, Bosque A, Chan J, Famiglietti M, Greene WC, Kashuba A, Lewin SR, Margolis DM, et al. An in-depth comparison of latent HIV-1 reactivation in multiple cell model systems and resting CD4+ T cells from aviremic patients. PLoS Pathog. 2013; 9:e1003834. [PubMed: 24385908]

Stevenson M, Stanwick TL, Dempsey MP, Lamonica CA. HIV-1 replication is controlled at the level of T cell activation and proviral integration. EMBO J. 1990; 9:1551–1560. [PubMed: 2184033]

Swanstrom R, Coffin J. HIV-1 pathogenesis: the virus. Cold Spring Harb Perspect Med. 2012; 2:a007443. [PubMed: 23143844]

Vandergeeten C, Fromentin R, Merlini E, Lawani MB, DaFonseca S, Bakeman W, McNulty A, Ramgopal M, Michael N, Kim JH, et al. Cross-clade ultrasensitive PCR-based assays to measure HIV persistence in large-cohort studies. J Virol. 2014; 88:12385–12396. [PubMed: 25122785]

HIGHLIGHTS

- HIV RNA and protein co-expression allows *ex vivo* characterization of patient CD4 T cells
- HIV-infected CD4s show markers of exhaustion and peripheral follicular helper cells
- Translation-competent latent reservoir can be detected in most ART-treated patients
- PKC agonist Bryostatin preferentially reactivates HIV from effector memory CD4s

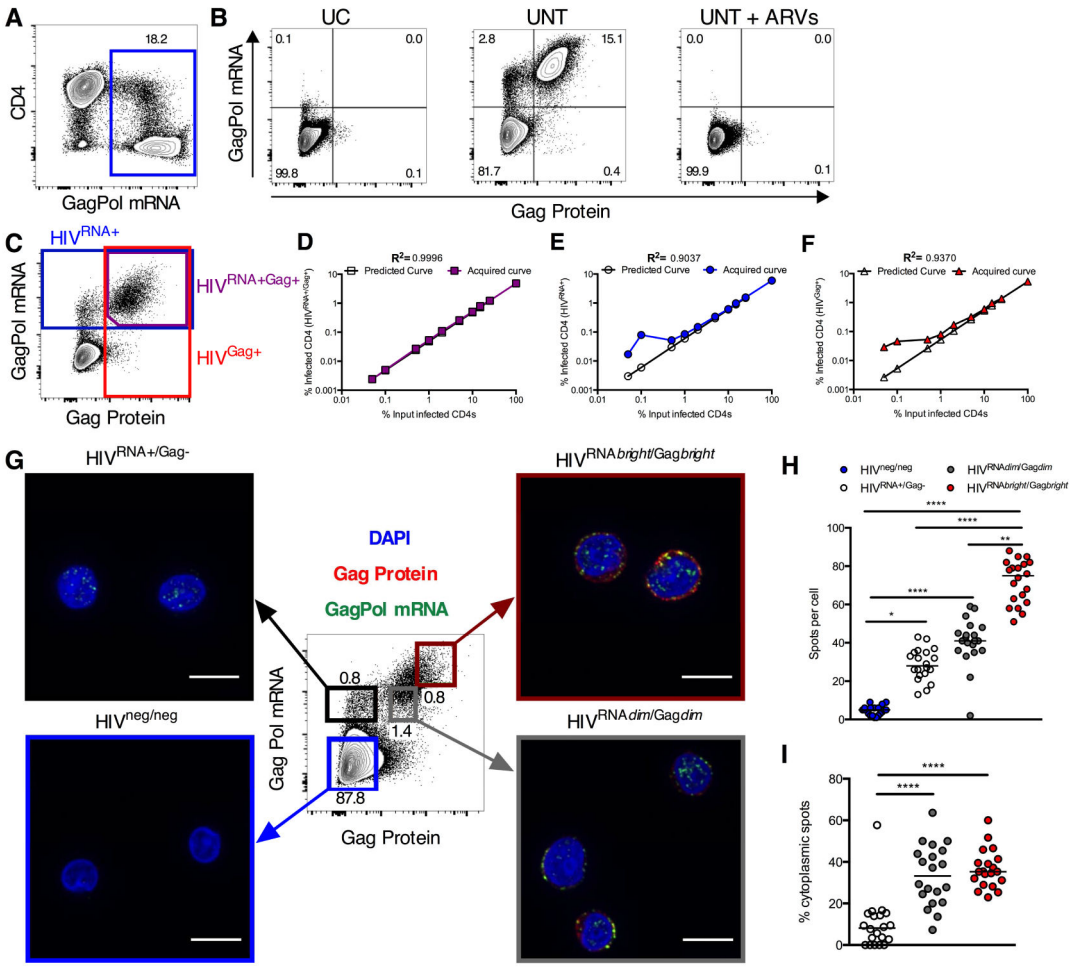

Figure 1. Dual staining for mRNA and protein allows highly sensitive, flow based detection and microscopy analysis of HIV-infected CD4

Peripheral CD4 from HIV-1-infected patients were activated *in vitro* and a spreading infection with endogenous virus established. (**A**) Example plot showing GagPol mRNA staining. (**B**) Example concurrent Gag protein and GagPol mRNA staining for an uninfected control (UC); a viremic patient (UNT) or UNT CD4 cultured with ARVs (UNT + ARVs). (**C–F**) HIV-infected CD4 were "spiked" into uninfected CD4 at different ratios. (C) Example gating of CD4 expressing GagPol mRNA and protein (purple), GagPol mRNA (blue) or Gag protein (red). Quantification of predicted (clear symbols) vs acquired result (colored symbols) using (D) double mRNA and protein expression, or single (E) mRNA or (F) protein stain. R^2 calculated on log-transformed data. (**G–I**) Reactivated, HIV-infected CD4 were sorted into four populations based on Gag protein and GagPol mRNA expression (indicated by colored boxes (**G**)) and imaged by confocal microscopy. In example images from sorted populations DAPI is in blue, GagPol mRNA in green and Gag protein in red. Scale bars represent 10μm. (**H** and **I**) GagPol mRNA spot analysis for sorted populations from (G). (H) GagPol mRNA spots per cell in sorted populations. (I) Frequency of cytoplasmic mRNA spots. Each symbol represents a cell. n=20 cells, representative data

from one donor. *p<0.05, **p<0.01, ***p<0.001 by Kruskal-Wallis ANOVA with Dunn's post-test. See also Figures S1, S2 and S3, Table S1 and Movies S1 and S2.

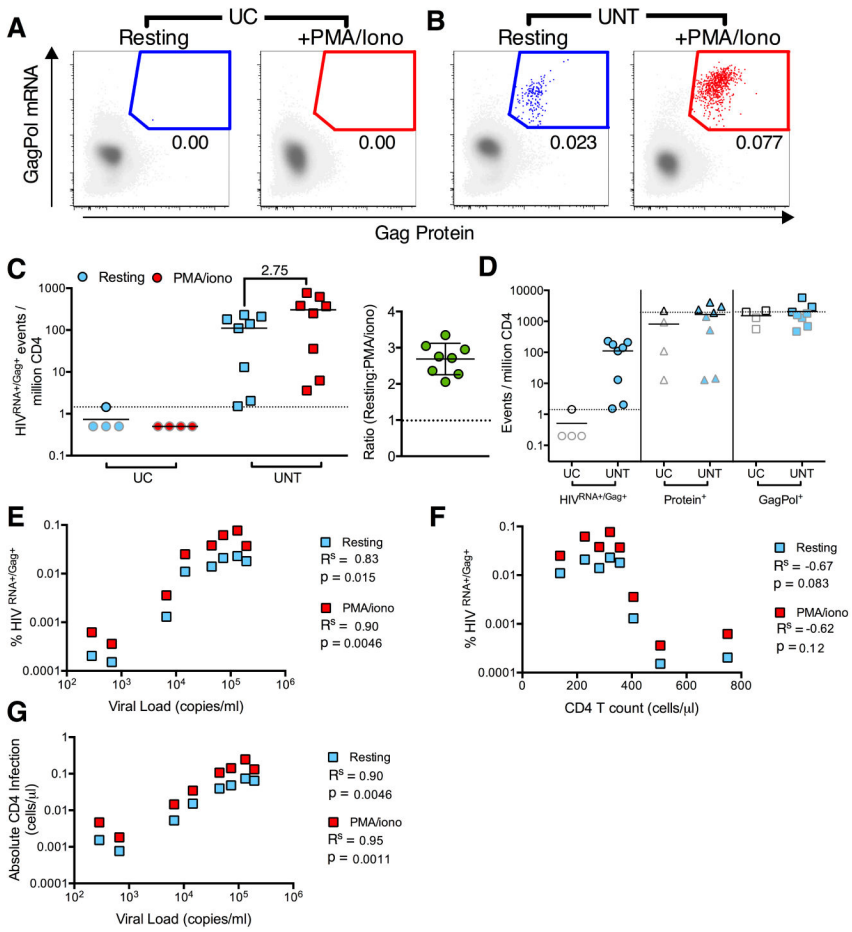

Figure 2. Detection of CD4 T cells supporting ongoing and activation-inducible HIV infection in viremic patients

$HIV^{RNA+/Gag+}$ CD4 were detected in uninfected controls (UC) or viremic patients (UNT) directly *ex vivo* (resting, blue symbols) or following 12 hr stimulation (PMA/iono, red symbols). (**A** and **B**) Example plots and gating of $HIV^{RNA+Gag+}$ CD4 for an UC (A) and an UNT (B). $HIV^{RNA+/Gag+}$ events in red/blue are overlaid onto $HIV^{neg/neg}$ events in gray. (**C** and **D**) Quantification of data in (AB), shown as $HIV^{RNA+/Gag+}$ events per million CD4 (n= 4 UC, 8 UNT). On right, the fold change in frequency of $HIV^{RNA+Gag+}$ CD4 in resting vs stimulated infection is shown. n= 8 UNT. (**D**) Data as in (C) for unstimulated, resting CD4, except gated using only protein ($Protein^{+}$) or mRNA ($GagPol^{+}$) staining, compared to $HIV^{RNA+/Gag+}$ staining. Limit of detection (LOD) based on frequency of UC false positive events is indicated with a dotted line. Grey-bordered symbols are below LOD. (**E–G**) Correlations of resting or stimulated infection with patient characteristics, (E) viral load (F) CD4 count or (G) absolute number of infected CD4 (CD4 count (cells/µl) × % $HIV^{RNA+/Gag+}$). R^{s} represents Spearman's non-parametric correlation with associated p values where $p<0.05$ is significant. See also Figure S4 and Table S2.

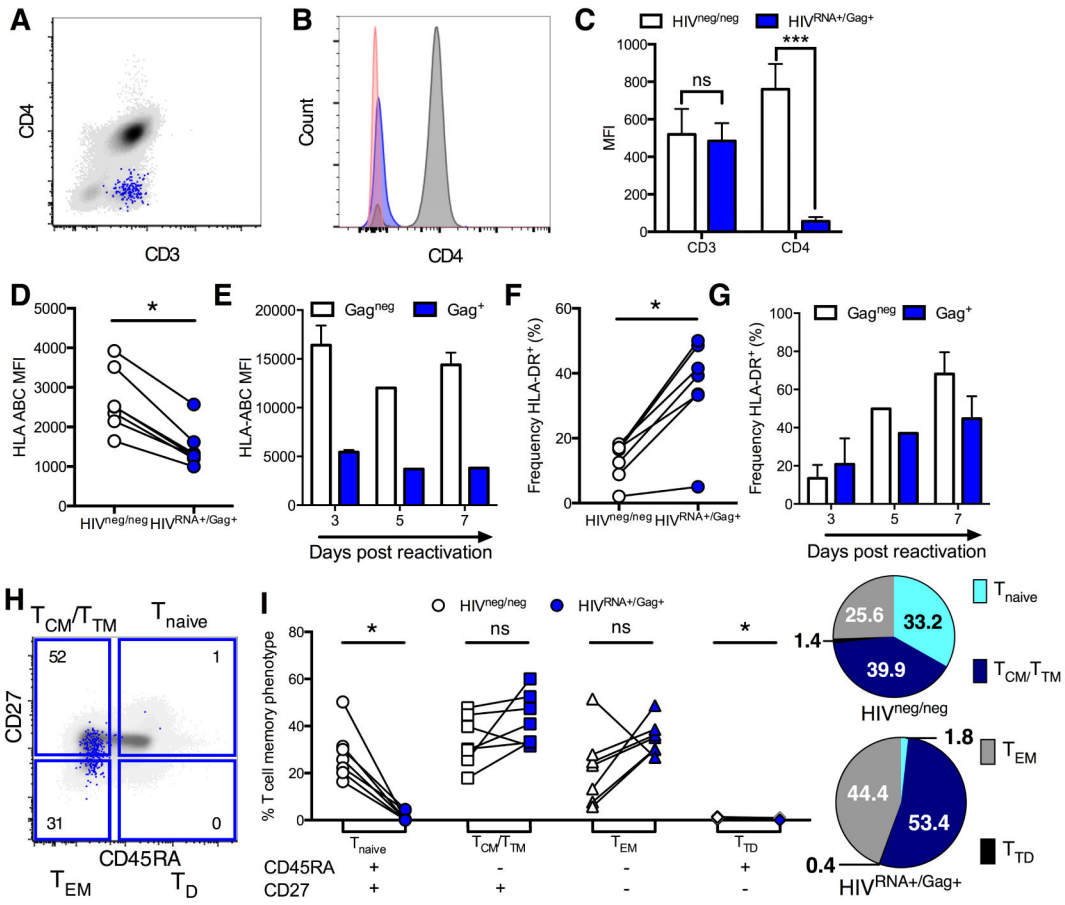

Figure 3. Dissociated expression patterns of CD4 co-receptors and memory phenotype of CD4 cells maintaining ongoing infection in viremic individuals

Peripheral CD4 from viremic, untreated (UNT) patients were analyzed directly *ex vivo* without stimulation for phenotype. White symbols/bars represent $HIV^{neg/neg}$ CD4 and blue represents $HIV^{RNA+/Gag+}$ CD4 from the same patient sample. (**A–C**) $HIV^{RNA+/Gag+}$ T cells downregulate CD4. (A) Example plot overlaying $HIV^{RNA+/Gag+}$ (blue) onto $HIV^{neg/neg}$ (gray) CD4. (B) Histogram of staining in (A) with negative control (red). (C) Quantification of results in (A and B). n=5 UNT. ***p<0.001 by Friedman ANOVA with Dunn's post-test. (**D–G**) HLA-ABC expression (D and E) and HLA-DR^+ frequency (F and G) on HIV-infected vs uninfected CD4. For D and F infected cells were defined by dual mRNA/protein stain on unstimulated UNT CD4 analyzed directly *ex vivo*. For E and G infected CD4 were defined by standard Gag protein staining only at time points post-reactivation for an endogenous, spreading infection. (**H** and **I**) Comparison of memory phenotype between $HIV^{RNA+/Gag+}$ CD4 in UNT compared to $HIV^{neg/neg}$ CD4. (H) Example plot and gating with $HIV^{RNA+/Gag+}$ CD4 (blue) overlaid onto total T cell population (grey). Numbers represent frequency of $HIV^{RNA+/Gag+}$ CD4 with specific phenotype. (I) Quantification of data in (H). Numbers shown in pie charts represent normalized mean. n=7 UNT, except in (E and G) where n=2. ns signifies p>0.05, *p<0.05 by Wilcoxon signed rank test. See also Figure S5.

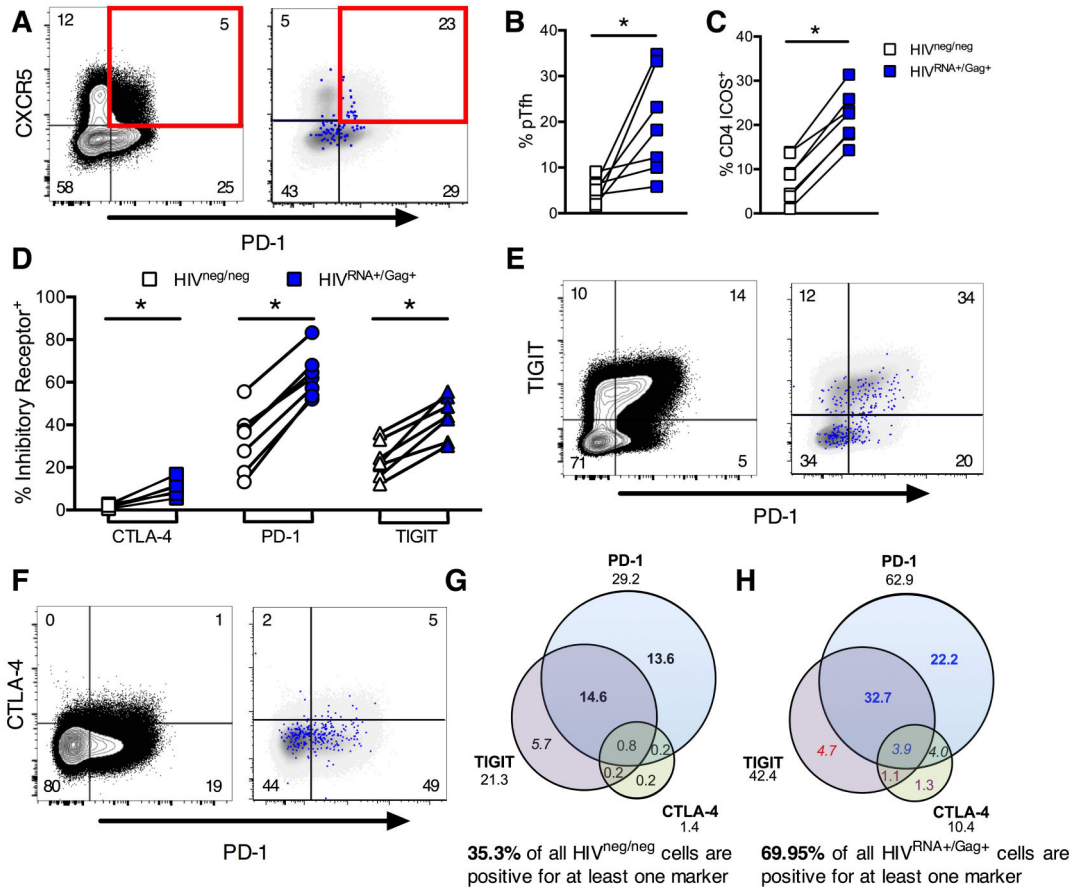

Figure 4. CD4 T cells maintaining ongoing replication during viremia show markers of activation, exhaustion and peripheral T follicular helper cells

Peripheral CD4 from viremic patients (UNT) were analyzed without stimulation for phenotype directly *ex vivo*. For example plots in **A, E** and **F**, left hand panel shows gating on total CD4 T cells with frequencies of each population indicated. Right hand panel shows $HIV^{RNA+/Gag+}$ CD4 events in blue, overlaid onto $HIV^{neg/neg}$ events (gray) for the same markers. Frequencies shown represent the $HIV^{RNA+/Gag+}$ population. (**A**) Example plots of pTfh phenotype (pre-gated on CD45RA-memory CD4). (**B**) Quantification of results in (A), shown as frequency of memory CD4. (**C**) Frequency of ICOS expression on $HIV^{RNA+/Gag+}$ versus $HIV^{neg/neg}$ CD4. (**D**) Relative expression of coinhibitory receptors CTLA-4, PD-1 and TIGIT on $HIV^{RNA+/Gag+}$ compared to $HIV^{neg/neg}$ CD4. (**E** and **F**) Example plots of coexpression; TIGIT and PD-1 (E), CTLA-4 and PD-1 (F). (**G** and **H**) Boolean analysis of inhibitory receptor coexpression on $HIV^{neg/neg}$ (G) vs $HIV^{RNA+/Gag+}$ (H) CD4 from the same patients. Numbers under inhibitory receptor name indicate total frequency of positive events (e.g. all $PD\text{-}1^{+}$) and correspond to data in (EF). Red text indicates populations under represented in $HIV^{RNA+Gag+}$ versus $HIV^{neg/neg}$. Populations enriched in $HIV^{RNA+Gag+}$ by 1–5-fold are blue, 5–10 fold (purple) or over 10 fold (black). Populations contributing more than 2 or 10% are in italics or bold respectively. Data represent medians. n=7 UNT. *$p<0.05$ by Wilcoxon signed rank test. See also Figure S5.

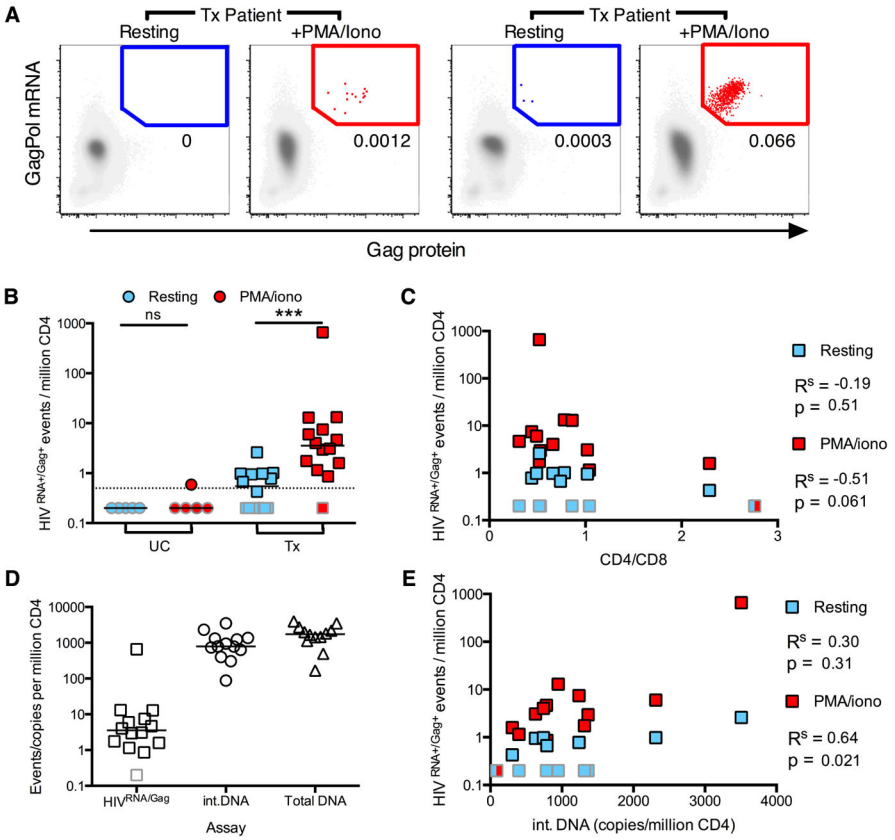

Figure 5. Detection of latently HIV-infected CD4 T cells from ART-treated patients

Peripheral $HIV^{RNA+Gag+}$ CD4 were detected in treated, aviremic patients (Tx) directly *ex vivo* (resting, light blue), or following stimulation (PMA/iono, red). (**A**) Example plots of a representative patient (left) or a patient with a large inducible reservoir (right). (**B**) Quantification of data in (A) for Tx and uninfected controls (UC). Dotted line represents limit of detection (LOD). ns signifies $p>0.05$, ***$p<0.001$ by Wilcoxon signed rank test. (**C**) Correlation between reactivation and CD4/CD8 T cell ratio. Where result is the same between two conditions, a split box is shown. (**D**) Comparison of reservoir measured by different techniques; $HIV^{RNA/Gag}$ assay (with PMA/iono stimulation, data as in (B)), integrated HIV DNA PCR (int.DNA) and total HIV DNA PCR. Line shown at median. (**E**) Correlation between reservoir as measured by integrated DNA and $HIV^{RNA/Gag}$ assays. Gray bordered symbols are below LOD. In all experiments, n=5 UC and 14 Tx (13 for Figure 5D and E). Statistics shown are Spearman's correlation coefficient (R^s) with associated p values. See also Figure S6 and Tables S3 and S4.

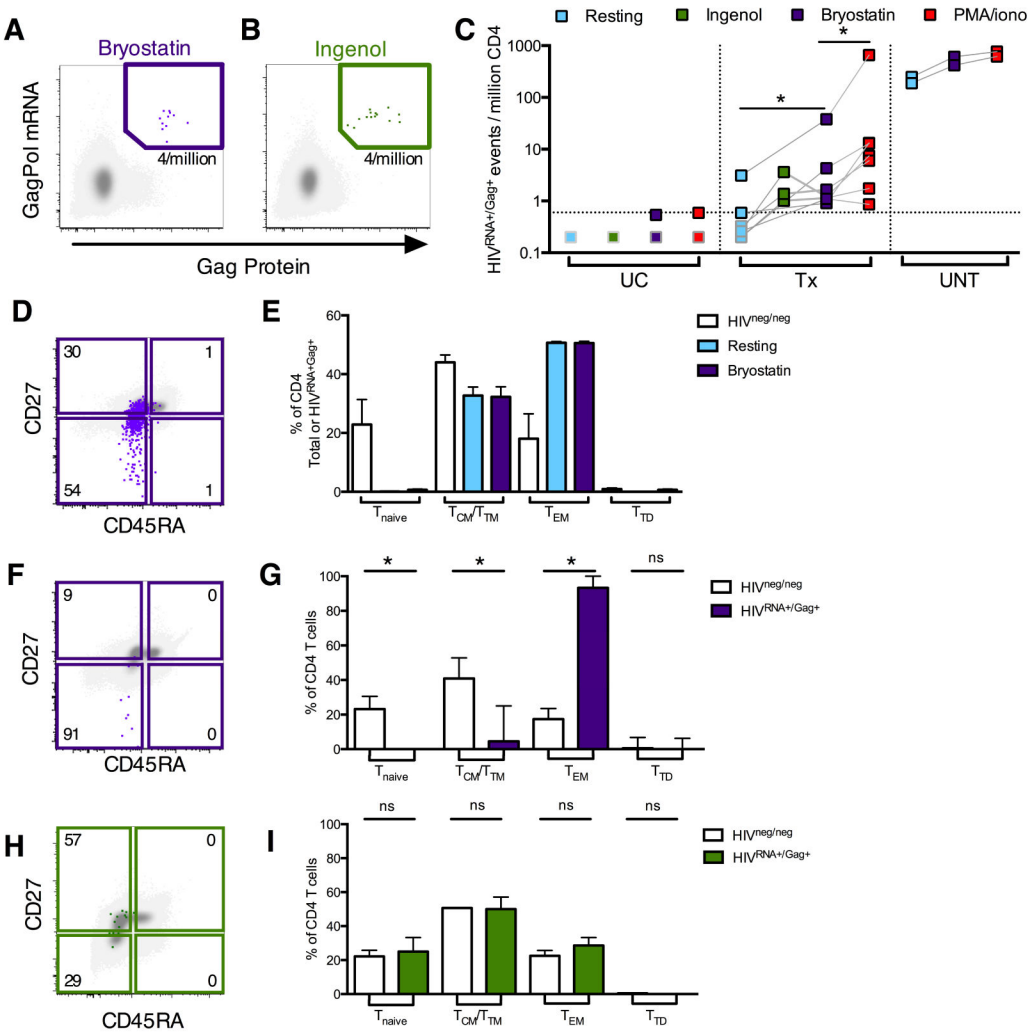

Figure 6. Quantification and phenotyping of LRA-reactivated infected CD4 cells in patients on or off ART

$HIV^{RNA+/Gag+}$ CD4 from UC, UNT or Tx patients were detected directly ex vivo (resting, light blue symbols/bars), or following reactivation with ingenol (green), bryostatin (purple) or PMA/iono (red). In example plots, reactivated $HIV^{RNA+/Gag+}$ events (green/purple) are overlaid onto $HIV^{neg/neg}$ events (gray). Frequencies of $HIV^{RNA+/Gag+}$ CD4 are indicated in each gate. (**AB**) Example plots for Tx patients following bryostatin (A) or ingenol reactivation (B). (**C**) Summary data of $HIV^{RNA+/Gag+}$ CD4 frequencies in unstimulated vs stimulated CD4. n=4 UC, 2 UNT and 3–7 Tx. Dotted line indicates LOD. Grey-bordered symbols are below LOD. (**D**) Example plot showing memory phenotype of bryostatin-reactivated $HIV^{RNA+/Gag+}$ CD4 for an example UNT. (**E**) Quantification of data in (D) for n=2 UNT, comparing $HIV^{neg/neg}$ with $HIV^{RNA+/Gag+}$ CD4, unstimulated or after bryostatin stimulation. $HIV^{neg/neg}$ CD4 are shown in white. Bars= mean±SEM. (**F**) Example plot showing memory phenotype of bryostatin-reactivated $HIV^{RNA+/Gag+}$ CD4 for a Tx patient. (**G**) Quantification of data in (F). n=7 Tx. (**H**) Example plot showing memory phenotype of ingenol-reactivated $HIV^{RNA+/Gag+}$ CD4 for a Tx patient. (**I**) Quantification of data in (H).

n=3 Tx patients. ns indicates $p>0.05$, *$p<0.05$ by Wilcoxon signed rank test. For G+I bars= median±interquartile range. See also Figure S6 and Table S3.